MDPI

Article

Liquid Loading of Horizontal Gas Wells in Changbei Gas Field

Zhimin Huang *, Wenbin Cai *[ID]**, Huiren Zhang and Xiangyang Mo**

College of Petroleum Engineering, Xi'an Shiyou University, No. 18, Electronic Second Road, Yanta District, Xi'an 710065, China

* Correspondence: zhiminhuang1997@163.com (Z.H.); caiwenbin@xsyu.edu.cn (W.C.)

Abstract: The Changbei gas field, which initially exhibited high gas-production performance, is dominated by large-displacement horizontal wells. With the decrease in reservoir pressure, the liquid loading in the gas well is currently severe, and production has been rapidly decreasing. Thus, recognizing the gas-well liquid loading to maintain stable gas-well production is necessary. A method was established to identify the water source of the liquid loading in the Changbei gas field. First, formation water and condensate water were identified based on the mineralization of the recovered water and the mass concentration of Cl^- and $K^+ + Na^+$, and then the condensate content of the water produced in the gas well was qualitatively evaluated. The water–gas ratio curve for the gas well was plotted to determine whether the produced water was edge-bottom water, pore water, or condensate. Then a method was established to distinguish the start time of liquid loading in the gas well using a curve depicting a decrease in production; the method was also used to estimate the depth of the gas well where liquid loading occurs, according to the bottomhole pressure. First, based on the available production data, the Arps decline model was applied to fit the production curve for the entire production phase; the resulting curve was compared with the actual production curve of the gas well, and the two curves diverged when fluid accumulation began in the gas well. Finally, the liquid-loading depth of the gas well was estimated based on the bottomhole pressure. This method can be used to determine the fluid accumulation and calculate the liquid-loading depth of gas wells with unconnected oil jackets. The analysis revealed that in the Changbei gas field, condensate was the type of water primarily produced in 35 gas wells, accounting for 62.5% of the total number of gas wells. Edge-bottom water was the type of water primarily produced in 16 gas wells, accounting for 28.6% of the total number of gas wells. In the remainder of the gas wells, pore water was the water primarily produced; the calculations of accumulation time and accumulation volume of typical gas wells in the block revealed that some gas wells started to accumulate liquid after 45–50 months, and the amount of accumulation could reach several tens of meters, while others were in good production condition. The method established in this paper could enhance our understanding of liquid loading in gas wells in the Changbei gas field and lay a foundation for the development of gas-well deliquification techniques.

Keywords: horizontal gas well; Changbei gas field; water source analysis; liquid loading

1. Introduction

The Changbei block, a typical "low-permeability, low-porosity" gas reservoir, is located on the Yishaan Slope in the north-central part of the Ordos Basin, with a porosity of 5–8% and a permeability of 0.7×10^{-3}–5×10^{-3} μm^2 (Figure 1). The study area is currently dominated by horizontal wells with open hole completions. Approximately half of these wells initially produced as much as 100×10^4 m^3/d per well; however, after years of exploitation, the liquid-loading capacity of several horizontal wells has decreased, and the gas cannot carry all the produced water out of the wellbore because of insufficient formation energy, resulting in liquid loading and a severe effect on the normal production of the gas wells [1–3]. Accurately identifying the water produced in the gas well and determining the gas-well liquid loading is crucial.
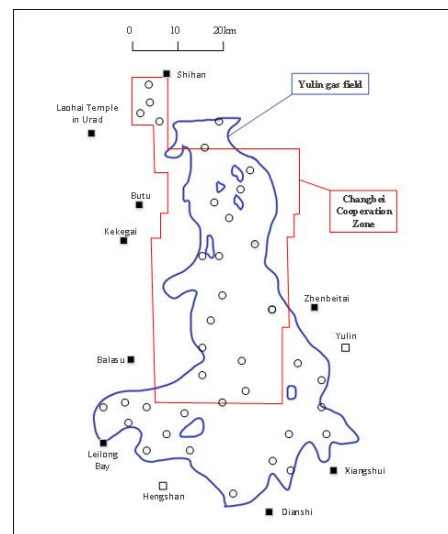
Figure 1. Location map of Changbei block.

The common methods currently used to diagnose liquid loading in horizontal gas wells include the differential pressure method, flow pressure testing method, and critical flow rate method [4–8]. Several studies have been conducted worldwide on gas-well liquid loading in recent years. Veeken et al. analyzed the influence of gas-phase velocity on liquid loading for different well parameters and proposed a modified Turner's critical liquid-carrying model [9]. Xiong yu et al. summarized the laws and characteristics of changes in wellhead oil pressure and daily gas production due to liquid loading in the Sulige gas field as a basis; accordingly, they determined whether fluid accumulation occurs in the gas wells [10]. Shekhar et al. assumed that liquid loading begins when the liquid film starts to fall and that the gas well diameter and inclination angle determines the time when liquid loading starts at different inclination angles [11]. Liu yonghui et al. visualized an experimental setup to simulate gas–liquid flow in a horizontal well. By recognizing the liquid-film reversal using a high speed camera, a series of experiments were conductedusing different angles, pipe sizes, and liquid flowing rates [12]. Wang zhibin et al. determined the friction coefficient at the gas–liquid interface and developed an analytical model to predict the state of gas-well liquid loading based on the force balance at the bottom of the inclined section [13]. However, most of the gas wells in the Changbei gas field are installed with packers in the annulus, and the oil casing is not connected; thus, the casing pressure does not reflect the production status at the bottom of the well. The flow pressure test method can be used to accurately determine the fluid level but is not cost effective and cannot be continuously monitored. The critical flow rate method was developed based on theoretical derivations and experimental studies with several differences between the models [14–17]. In this study, the water-production type of horizontal gas wells was classified according to the water-production characteristics and the water chemistry of the gas wells in the Changbei block. According to actual production data, a method was developed to determine the time of gas-well liquid loading based on a curve of production decrease and to estimate the depth of the gas-well liquid loading based on bottomhole flow pressure. This method can be used easily and quickly to obtain the time when the gas well starts to accumulate and estimate the volume of liquid loading in the gas well, which is temporarily not available in the current methods used to diagnose liquid loading in horizontal gas wells. Of course, there are also many problems, which cannot be solved due to the limitations of the stage.

2. Analysis of the Source of Produced Water

Water produced in gas wells may have multiple sources, and different sources of produced water have different production and water chemistry characteristics. The source

of produced water in the Changbei block may include formation water, condensate water, or a mixture of both [18,19]. These types of water sources can be effectively identified through the integrated discrimination of mineralization, analysis of the water–gas ratio, and calculation of the water content in the gas well.

2.1. Water Analysis for Water-Source Identification

Table 1 displays the physical characteristics of various types of produced water. The fluid characteristics of condensate and formation water are considerably different in terms of mineralization, which is the most direct and effective technique to determine the source of water in gas wells [20,21].

Table 1. Physical characteristics of effluent.

Type of Water Production	Fluid Properties
Edge-bottom water	High mineralization, with total mineralization of approximately 5×10^4–7.52×10^4 mg/L, and high mass concentrations of Cl^-, $K^+ + Na^+$, and other ions
Pore water	
Condensate	Low mineralization, with total mineralization of approximately 0.2×10^4–0.6×10^4 mg/L, and low mass concentrations of Cl^-, $K^+ + Na^+$, and other ions

The analysis of water samples from the wellheads of water-producing gas wells in the Changbei gas field revealed that the degree of mineralization was generally low; 0.5×10^4 mg/L was selected as the mineralization degree cut-off point for condensate water in this block; and 2×10^4 mg/L was selected as the mineralization degree cut-off point for formation water. Ten of these wells were selected for water source discrimination (Table 2).

Table 2. Aqueous parameters of gas-well-produced water.

Well Number	Mineralization Degree /(mg/L)	CL^- Mass Concentration /(mg/L)	$K^+ + Na^+$ Mass Concentration /(mg/L)	Source of Produced Water
CX-1	7982	730	2216	Not certain
CX-2	19,278	10,227	4292	Stratigraphic water
CX-3	3148	1419	1158	Condensate
CX-4	11,928	720	3846	Not certain
CX-5	3613	1095	836	Condensate
CX-6	802	270	196	Condensate
CX-7	3879	360	894	Condensate
CX-8	25,867	12,419	4522	Stratigraphic water
CX-9	5974	709	1987	Not certain
CX-10	2367	733	799	Condensate

2.2. Qualitative Evaluation Method for Gas Condensate Content

Condensate is typically composed of natural gas with saturated steam in a gaseous state or as mist droplets under formation conditions; it condenses into water because of decompression and a temperature decrease at the wellhead. The condensates are distinct and are typically accompanied by a small amount of water and formation water, which produces a large amount of water.

As displayed in Table 2, the wells CX-1, CX-4, and CX-9 could not be identified by relying only on the mineralization of the water samples; therefore, the condensate content was qualitatively evaluated to further determine the water source. The theoretical condensate volume of the output was determined according to the variation in condensate content in the natural gas in the formation and wellhead states; the following equation was used:

$$q_{w1} = q_g \left(W_{WH_2O} - W_{TH_2O} \right) / \rho_w \tag{1}$$

where q_{w1} is the theoretical condensate volume of the gas well, m^3/d; q_g is the gas-production volume of the gas well, m^3/d; W_{WH_2O} is the saturated-steam volume of the natural gas at bottomhole pressure and temperature, kg/m^3; W_{TH_2O} is the saturated-steam volume of natural gas at wellhead pressure and temperature, kg/m^3; ρ_w is the density of condensate at wellhead conditions, kg/m^3. W_{WH_2O} and W_{TH_2O} can be calculated through the Mcketta–Wehe plot method [22,23].

The theoretical condensate volume q_{w1} was obtained using Equation (1), and the volume q_{w2} of the actual water produced at the wellhead was determined and compared with q_{w1} to determine the type of produced water. Table 3 illustrates large differences between the theoretical condensate volume and the actual volume produced in CX-1 and CX-4, which primarily produce formation water; CX-9 has a similar theoretical condensate volume and actual produced volume.

Table 3. Composition of the water produced in the gas wells.

Well Number	$W_{WH_2O}-W_{TH_2O}$ /(10^{-3} kg/m^3)	q_g/(10^6 m^3/d)	q_{w1}/(m^3/d)	q_{w2}/(m^3/d)	Type of Water Production
CX-1	1.35	0.17	0.229	1.35	Formation water dominates
CX-4	1.01	0.30	0.304	2.32	Formation water dominates
CX-9	1.2	0.6	0.72	0.80	Condensate based

2.3. Water Source Identification Based on Effluent Characteristics

The formation water is further divided into edge-bottom water and pore water. Table 4 displays the characteristics of the various types of water produced as reported by previous studies [24]. The characteristics of the edge-bottom water, pore water, and condensate water are notably different. By analyzing the variation of the produced water–gas ratio, we can quickly distinguish between edge-bottom water and pore water.

Table 4. Characterization of water produced in the gas wells.

Type of Produced Water	Characteristics of Produced Water
Edge-bottom water	High water production and unstable water–gas ratio indicate an up and down fluctuation or a sharp rise
Pore water	Large differences in regional water production and stable water–gas ratio, typically less than 0.5 m^3/10^4 m^3
Condensate	Stable and considerably low water–gas ratio

The dynamic water–gas ratio curves for the CX-2 and CX-8 (Figure 2) indicated that although the water–gas ratio of the CX-2 well did not exceed 0.5 m^3/10^4 m^3, the water production and water–gas ratio exhibited a rapid increasing trend within a short period of time, indicating that water intrusion had started to occur in the gas well [25]. Similar results were obtained for the CX-8 well, indicating that both produce edge-bottom water.
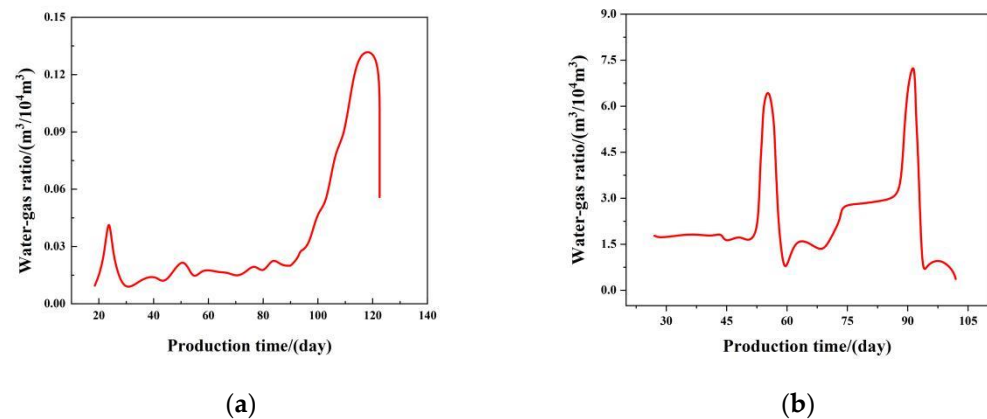
(**a**)   (**b**)

Figure 2. Production time vs. dynamic water–gas ratio curves for the CX-2 and CX-8 wells. (**a**) CX-2 gas well. (**b**) CX-8 gas well.

2.4. Comprehensive Analysis

Applying the above discriminative methods, the produced water of Changbei gas field was classified into three types: condensate, edge-bottom water, and pore water.

In the gas field, condensate was the type of water primarily produced in 35 gas wells, accounting for 62.5% of the total number of gas wells. Edge-bottom water was the water primarily produced in 16 gas wells, accounting for 28.6% of the total number of gas wells. In the remainder of the gas wells, pore water was the water primarily produced. If new horizontal gas wells are drilled in the Changbei gas field in the future, the type of produced water in the new wells can be determined based on Table 5.

Table 5. Classification of water production types of gas reservoirs in the Changbei gas field.

Source of Produced Water	Total Mineralization (mg/L)	Output Mechanism	Water–Gas Ratio ($m^3/10^4\ m^3$)	Impact on Gas Well Production	Whether Deliquification Occurred
Condensate	Low mineralization, typically less than 0.5×10^4 mg/L	Mixed with natural gas in a single gas phase, produced with natural gas production	Stable and very low	Basically no effect	No
Edge-bottom water	High mineralization, approximately 2×10^4 mg/L	High water production	Unstable, fluctuates up and down or sharply increases	Rapid rise in water production and high impact on gas-well production	Yes
Pore water		Large differences in regional water production	Stable	There is some impact when the water volume is high	Drainage is required when the water volume is large

3. Analysis of Wellbore Liquid Loading

To solve the problem of gas-well liquid loading, liquid loading in the gas well must be diagnosed. In this study, we established a method that combines the analyses of decreasing production and bottomhole inflow performance to determine gas-well liquid loading according to the actual production data of gas wells through the following steps.

(1) A curve for decreasing production is fitted according to the production data when liquid loading does not occur in the gas well to obtain a rating curve between production q_1

and the time required for the entire production phase when liquid loading does not occur in the gas well.

(2) A rating curve is plotted between actual production q_2 and time.

(3) The fluctuation of q_2 up and down around the rating curve of q_1 indicates that the well is in a good production state. Large differences between q_1 and q_2 for a long time occur because of liquid loading by produced water. Bifurcation occurs when the liquid loading begins.

(4) When bifurcation begins, the bottomhole pressures P_{w1}, corresponding to q_1, and P_{w2}, corresponding to q_2, are determined based on the correlation between gas production and bottomhole pressure on the IPR curve. The difference between the two bottomhole pressures is equal to the pressure generated by the column of gas-well liquid loading, and the depth of liquid loading is estimated.

3.1. Time of Liquid-Loading Initiation

In 1945, Arps [26] devised three laws to explain the decrease in gas production based on the definition. Considering the loss ratio, only three parameters in the equation (initial decreasing yield q_i, decreasing index b and initial decreasing rate D_i) are required to predict the future yield q (Table 6).

Table 6. Three decreasing yield equations.

Decreasing Type	Decreasing Index	Yield–Time Relationship
Index	b = 0	$q = q_i e^{-D_i t}$
Hyperbolic	0 < b < 1	$q = \dfrac{q_i}{(1+bD_i t)^{1/b}}$
Harmonization	b = 1	$q = \dfrac{q_i}{1+D_i t}$

Using the equation for the relationships between production and time listed in Table 6, three types of curves depicting the decrease in production were obtained by fitting the production data when liquid loading did not occur in the gas well. Comparing the three types of curves, the one with the highest fit R^2 was selected, and the data were used to obtain the predicted rating curve between production q_1 and the time required for the entire production phase when liquid loading does not occur in the gas well. The rating curve between actual production q_2 and time was also plotted and the two curves were compared. If q_2 fluctuates up and down around the rating curve of q_1, the well exhibits good production performance; the large differences between the two over time are most likely because of liquid loading of the produced water. This indicates the initiation of gas-well liquid loading.

3.2. Calculation of Liquid-Loading Depth

When liquid loading occurs in a gas well, a difference is observed between the bottomhole pressure P_{w1} corresponding to q_1, which is obtained from the fit of the decrease in production during the entire production phase of the gas well, and the bottomhole pressure P_{w2}, corresponding to actual production q_2. According to the law of conservation of energy, the pressure loss is primarily caused by wellbore friction, gas acceleration, and liquid-column pressure. Under stable production conditions, the decrease in pressure due to gas acceleration is basically negligible. Furthermore, under the same formation-pressure and wellhead-pressure conditions, a similar decrease in pressure is caused by the wellbore friction and by the gravity of the gas [27–29], but the liquid-column pressure is different in both cases. The depth of liquid loading is calculated using the following equation [30]:

$$H = \frac{P_{w1} - P_{w2}}{\rho_w g} \tag{2}$$

where P_{w2} is the bottomhole pressure corresponding to the actual production q_2, MPa; P_{w1} is the bottomhole pressure corresponding to the fitted production q_1, MPa; ρ_w is the density

of produced water; P_{w1} and P_{w2} are obtained according to the IPR curves of the well at two different productions q_1 and q_2.

3.3. Application Examples

Four horizontal gas wells in the Changbei block were selected to analyze wellbore liquid loading using the aforementioned method. The production data of these gas wells revealed that the production of these wells was not consistent, they had several shut-in points, and fluctuated notably. Therefore, to determine the trend of the decrease in production, all shut-in points were removed, and the cumulative production of 30 days was used as a unit of measurement.

Based on the screened and processed production data, the classical Arps decline law and the non-liquid production data were applied to obtain the curves for the decrease in production of these four horizontal gas wells. Furthermore, the actual production data and predicted production data were combined in one graph as shown in Figure 3.
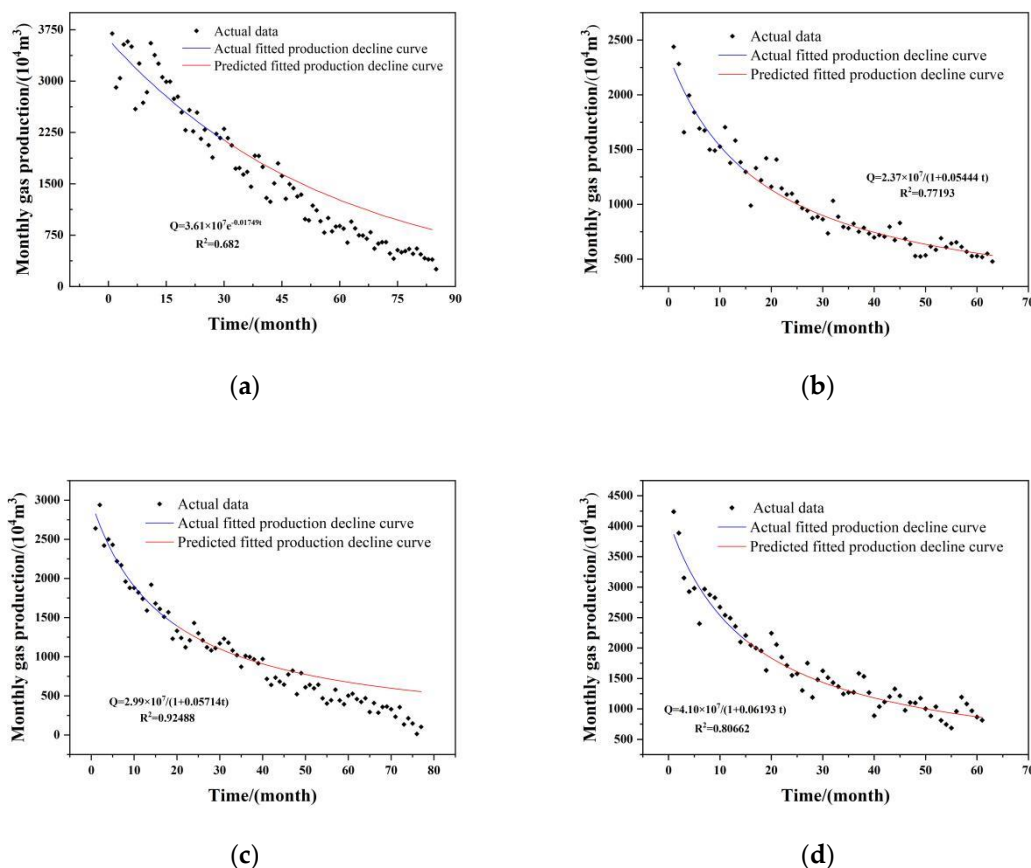

Figure 3. Curves of production decline and actual production of typical gas wells in the Changbei block. (**a**) Well CX-2. (**b**) Well CX-5. (**c**) Well CX-6. (**d**) Well CX-10.

The actual production of well CX-2 in the middle period fluctuated up and down around the production curve fitted, as explained by the production decline law. However, after 45 months of production, the actual production of the well is lower than that calculated according to the production decline law. Thus, liquid loading in the well was estimated to begin after the first 45 months. The actual production of well CX-5 and well CX-10 fluctuated up and down around the production curve fitted by the law of production decline, indicating that the well had good production performance. The actual production of well CX-6 fluctuated up and down around the production curve fitted by the production decline law in the middle of the period, but after 50 months of production, the actual

production of the well was lower than that calculated according to the production decline law; thus, liquid loading in the well started after 50 months.

Based on Equation (2), as displayed in Figure 4, the depth of the initial liquid loading in the well CX-2 was estimated to be approximately 39.7 m, and the depth of the initial liquid loading in well CX-6 was estimated to be approximately 86.7 m.
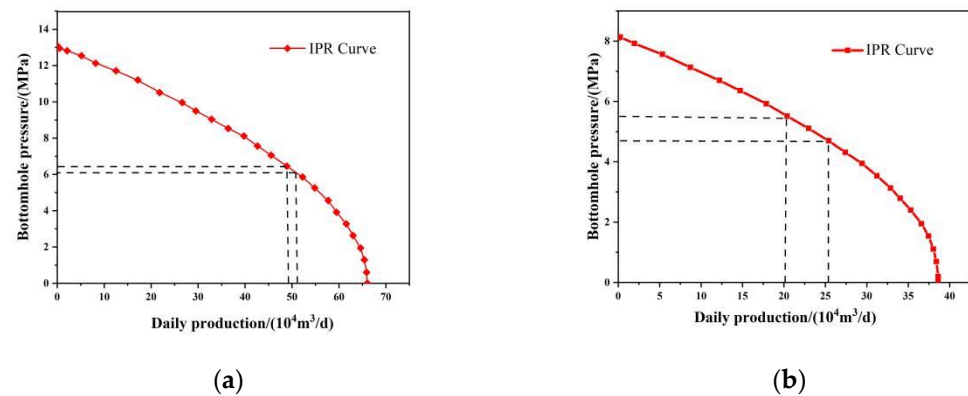

(**a**)　　　　　　　　　　　　　　　　　　　(**b**)

Figure 4. IPR curves of typical gas wells in the Changbei block. (**a**) Well CX-2. (**b**) Well CX-6.

4. Conclusions

The source of the produced water in the gas wells in the Changbei block was initially determined by analyzing the mineralization of the water samples and further determined through the theoretical calculation of water content and the analysis of the produced water's characteristics. Then analyses of the decrease in production and bottomhole inflow performance can help determine whether liquid loading occurred in the wells and calculate the depth of liquid loading. The results indicated that in the Changbei gas field, condensate was the type of water primarily produced in 35 gas wells, accounting for 62.5% of the total number of gas wells. Edge-bottom water was the water primarily produced in 16 gas wells, accounting for 28.6% of the total number of gas wells. In the remainder of the gas wells, pore water was the water primarily produced; if new horizontal gas wells are drilled in the Changbei gas field in the future, the type of water produced in the new wells can be determined. Some gas wells started to accumulate liquid after 45–50 months, and the amount of accumulation could reach several tens of meters, while others were in good production condition. Some of the other study methods, including the differential pressure method, flow pressure testing method, and critical flow rate method, have extremely high costs and some of them are based on empirically developed models, which are not very applicable and produce large errors. The method proposed in this paper is simple and rapid compared with them, but it also has some limitations, as it only has a general range for the time of liquid loading and cannot be accurate to a certain date. This should be a key concern for future research. Future research will hopefully combine accuracy with convenience.

Conflicts of Interest: The authors declare no conflict of interest.

References

1. Dong, H.; Wu, M.; Cui, G.; Dong, H.; Jiang, Z.; Chen, L.; Xu, J. Analysis and countermeasures of CB3-3 well low production causes. *Drill. Prod. Technol.* **2015**, *38*, 38–40.
2. Li, J.; Yang, B.; Chen, Z.; Yang, C.; Zhao, W. Reservoir protection technology in the Changbei gas field, Ordos basin. *Nat. Gas Ind.* **2009**, *29*, 68–70+138–139.
3. Zhao, X.; Lin, H.; Chen, L.; Tu, H.; Song, Y. Application of anti-sloughing drilling fluid technology to the long horizontal coalbed interval of well CB21-2. *Nat. Gas Ind.* **2012**, *32*, 81–85, 131–132.
4. Andrianata, S.; Allo, K.R.; Lukman, A.; Kramadibrata, A.T. Extending Life of Liquid Loaded Gas Wells Using Velocity String Application: Case Study & Candidate Selection. In Proceedings of the SPE/IATMI Asia Pacific Oil and Gas Conference and Exhibition 2017, Jakarta, Indonesia, 17–19 October 2017. [CrossRef]
5. Pagou, A.L.; Wu, X. Liquid Film Mode for Prediction and Identification of Liquid Loading in Vertical Gas Wells. In Proceedings of the International Petroleum Technology Conference, Dhahran, Kingdom of Saudi Arabia, 13–15 January 2020. [CrossRef]
6. Pagou, A.L.; Han, G.; Peng, L.; Dehdah, O.; Kamdem, V.G.; Abimbola, F.; Mccarthy, S.A.; Tchomche, H.F.; Harmash, I.; Kanturina, Z. Liquid loading prediction and identification model for vertical and inclined gas wells. *J. Nat. Gas Sci. Eng.* **2020**, *84*, 103641. [CrossRef]
7. Wang, R.; Ma, Y.; Dou, L.; Cheng, J.; Zhang, N. Review of critical liquid unloading rate models and liquid loading models for gas well producing water. *Sci. Technol. Eng.* **2019**, *19*, 10–20.
8. Xiao, C.Y.; Fu, H.; Cheng, L.L.; Pei, W.Y. Prediction of critical liquid loading time for water-producing gas wells: Effect of liquid drop rotation. *J. Pet. Explor. Prod. Technol.* **2021**, *12*, 1541–1548. [CrossRef]
9. Veeken, C.A.; Hu, B.; Schiferli, W. Transient Multiphase Flow Modeling of Gas Well Liquid Loading. In Proceedings of the SPE Offshore Europe Oil and Gas Conference and Exhibition, Aberdeen, UK, 8–11 September 2009. [CrossRef]
10. Xiong, Y.; Liu, B.; Xu, W.; Tan, B.; Huang, Y. Two Simple Approaches to Accurately Estimate Liquid Loading Quantity in Low—productivity Low—permeability Gas Producer. *Spec. Oil Gas Reserv.* **2015**, *22*, 93–96, 155.
11. Shekhar, S.; Kelkar, M.; Hearn, W.J.; Hain, L.L. Improved Prediction of Liquid Loading in Gas Wells. *SPE Prod. Oper.* **2017**, *32*, 539–550. [CrossRef]
12. Liu, Y.; Ai, X.; Luo, C.; Liu, F.; Wu, P. A new model for predicting critical gas velocity of liquid loading in horizontal well. *J. Shenzhen Univ. Sci. Eng.* **2018**, *35*, 551–557. [CrossRef]
13. Wang, Z.; Guo, L.; Zhu, S.; Nydal, O.J. Prediction of the Critical Gas Velocity of Liquid Unloading in a Horizontal Gas Well. *SPE J.* **2017**, *23*, 328–345. [CrossRef]
14. Coleman, S.B.; Clay, H.B.; McCurdy, D.G.; Norris, L.H.I. A New Look at Predicting Gas-Well Load-Up. *J. Pet. Technol.* **1991**, *43*, 329–333. [CrossRef]
15. Flores-Avila, F.S.; Smith, J.R.; Bourgoyne, A.T., Jr.; Bourgoyne, D.A. Experimental Evaluation of Control Fluid Fallback During Off-Bottom Well Control: Effect of Deviation Angle. In Proceedings of the IADC/SPE Drilling Conference, Dallas, TX, USA, 26–28 February 2002; p. SPE-74568-MS.
16. Li, M.; Guo, P.; Tan, G. New look on removing liquids from gas wells. *Pet. Explor. Dev.* **2001**, *28*, 100–110.
17. Turner, R.G.; Hubbard, M.G.; Dukler, A.E. Analysis and Prediction of Minimum Flow Rate for the Continuous Removal of Liquids from Gas Wells. *J. Pet. Technol.* **1969**, *21*, 1475–1482. [CrossRef]
18. Li, T.; Yang, W.; Li, D.; Xing, P.; Liu, Y.; Zhao, X.; Cao, G.; Bi, X. Synthesis and Plugging Mechanism of New Water-Swellable Rubber Particles for Fractured Pores in High Water-Cut Reservoirs. *Processes* **2022**, *10*, 2469. [CrossRef]
19. Yan, W.; Qi, Z.; Yuan, Y.; Huang, X.; Li, J. Influencing factor analysis of water invasion in condensate gas reservoir with bottom water based on fuzzy comprehensive evaluation and orthogonal experiment. *Geosystem Eng.* **2019**, *22*, 299–309. [CrossRef]
20. Liu, H.; Dong, J.; Cui, Y.; Liao, X.; Dai, Z.; Liu, Y.; Ning, B. Study on the law of aqueous phase changes and the origin of water production in gas wells. *Drill. Prod. Technol.* **2011**, *34*, 52–54, 115.
21. Sun, L.; Luo, J.; Zhang, J.; Xie, W.; Liu, J.; Wei, J. Method optimization for determining the water vapor contents in the natural gas of ultrahigh-pressure gasfields. *Pet. Geol. Oilfield Dev. Daqing* **2016**, *35*, 82–88.
22. McKetta, J.J.; Wehe, A.H. Use this chart for water content of natural gases. *Pet. Refin.* **1958**, *37*, 153–154.
23. Zhu, L.; Wang, B. Water content estimation of natural gas. *Nat. Gas Ind.* **1995**, *15*, 57–61, 101.
24. Du, M.; Wu, C.; Zhang, S.; Liu, X. Evaluation of the Geochemical Characteristics and Exploitation Potential of Produced Water from Coalbed Methane Wells in Eastern Yunnan, China. *J. Nanosci. Nanotechnol.* **2021**, *21*, 591–598. [CrossRef]
25. Si, L.; Xi, Y.; Wang, H.; Wen, Z.; Li, B.; Zhang, H. The influence of long-time water intrusion on the mineral and pore structure of coal. *Fuel* **2021**, *290*, 119848. [CrossRef]
26. Arps, J.J. Analysis of Decline Curves. *Trans. AIME* **1945**, *160*, 228–247. [CrossRef]

27.	Li, R.; Sun, Q.; Ding, X.; Zhang, Y.; Yuan, W.; Wu, T. Review of Flow-Matching Technology for Hydraulic Systems. *Processes* **2022**, *10*, 2482. [CrossRef]
28.	Liu, Y.; Cao, Y.; Wang, L.; Luo, C.; Wang, X.; Lu, G.; Ye, C.; Yang, J. Pressure drop model of gas-water-oil three-phase flow in horizontal gas wells. *Fault-Block Oil Gas Field* **2022**, *29*, 404–410.
29.	Yue, P.; Yang, H.; He, C.; Yu, G.M.; Sheng, J.J.; Guo, Z.L.; Guo, C.Q.; Chen, X.F. Theoretical Approach for the Calculation of the Pressure Drop in a Multibranch Horizontal Well with Variable Mass Transfer. *ACS Omega* **2020**, *5*, 29209–29221. [CrossRef]
30.	Yang, Z.; Zhao, C.; Liu, X.; Li, J.; Huang, C. Judgment of liquid loading and its depth calculation in the Dalaoba gas condensate field. *Nat. Gas Ind.* **2011**, *31*, 62–64, 136–137.